Mathematical Biosciences and Engineering

MBE, 20(5): 9349–9363.
DOI: 10.3934/mbe.2023410
Received: 09 January 2023
Revised: 22 February 2023
Accepted: 28 February 2023
Published: 17 March 2023

http://www.aimspress.com/journal/MBE

Research article

Automatic detection method of epileptic seizures based on IRCMDE and PSO-SVM

Bei Liu[1,2,*], Hongzi Bai[1], Wei Chen[1], Huaquan Chen[1] and Zhen Zhang[3]

[1] College of Mathematics and Physics, Hunan University of Arts and Science, Changde 415000, China
[2] Hunan University of Arts and Science, Hunan Province Key Laboratory of Photoelectric Information Integration and Optical Manufacturing Technology, Changde 415000, China
[3] Furong College, Hunan University of Arts and Science, Changde 415000, China

* **Correspondence:** Email: liubei@huas.edu.cn.

Abstract: Multi-scale dispersion entropy (MDE) has been widely used to extract nonlinear features of electroencephalography (EEG) signals and realize automatic detection of epileptic seizures. However, information loss and poor robustness will exist when MDE is used to measure the nonlinear complexity of the time sequence. To solve the above problems, an automatic detection method for epilepsy was proposed, based on improved refined composite multi-scale dispersion entropy (IRCMDE) and particle swarm algorithm optimization support vector machine (PSO-SVM). First, the refined composite multi-scale dispersion entropy (RCMDE) is introduced, and then the segmented average calculation of coarse-grained sequence is replaced by local maximum calculation to solve the problem of information loss. Finally, the entropy value is normalized to improve the robustness of characteristic parameters, and IRCMDE is formed. The simulated results show that when examining the complexity of the simulated signal, IRCMDE can eliminate the issue of information loss compared with MDE and RCMDE and weaken the entropy change caused by different parameter selections. In addition, IRCMDE is used as the feature parameter of the epileptic EEG signal, and PSO-SVM is used to identify the feature parameters. Compared with MDE-PSO-SVM, and RCMDE-PSO-SVM methods, IRCMDE-PSO-SVM can obtain more accurate recognition results.

Keywords: epilepsy; EEG signals; improved refined composite multi-scale normalized dispersion entropy; particle swarm algorithm; support vector machine

1. Introduction

Epilepsy is a common nervous system disease with sudden and irregular characteristics. At present, about 65 million people worldwide suffer from epilepsy, accounting for 1–2% of the world population [1]. Electroencephalography (EEG) is cheap, safe, and high-resolution, and is often used in the diagnosis of epilepsy [2–4]. In clinical practice, neurologists need to monitor patients' EEG records for a long time to identify normal, epileptic interictal, and epileptic ictal patterns [5]. However, this method of diagnosing epilepsy by analyzing EEG signals manually is a subjective and tedious process. Therefore, automatic detection of epileptic EEG signals will help reduce the workload of medical staff and provide a rapid response to emergencies [6–8].

Automated seizure detection methods are developed to distinguish between normal, epileptic interictal, and epileptic ictal EEG signals. Feature extraction from EEG signals using appropriate signal processing techniques is crucial for identifying epileptic seizure states, as the extracted features determine classification performance. Then, various machine learning algorithms are used to classify the extracted features [9]. So far, scholars in the field of epileptic diagnosis have tried to analyze epileptic EEG signals from a nonlinear perspective, and found that entropy characteristics can directly detect the dynamic changes of epileptic EEG signals [10–13]. Entropy is reported to be different for normal EEG signals and pathological seizure EEG signals, so it can effectively classify normal subjects and epileptic patients [14–16]. In literature [17–20], multiscale approximate entropy (MAE), multiscale sample entropy (MSE), and multiscale fuzzy entropy (MFE), as features of EEG signal, were used to distinguish normal, epileptic interictal, and epileptic ictal states. However, all these entropies above have the disadvantages of complicated calculation, high time consumption and not being suitable for real-time detection. Therefore, multiscale permutation entropy (MPE) was proposed by Bandt et al. to measure the nonlinearity of signals [21]. In literature [22], MPE was employed for epileptic feature extraction from EEG signals to complete the automatic detection of epilepsy. Despite MPE possessing the virtue of uncomplicated computation and fast computation speed [23–25], only the order of the coarse-grained sequence is considered in the time series analyzed by MPE, while amplitude information is ignored [26–28]. To overcome the above problems, Azami and Rostaghi et al. [29] proposed a nonlinear calculation method of multi-scale dispersion entropy (MDE), which not only has the virtue of uncomplicated computation and fast computation speed but also takes into account signal amplitude information when evaluating the non-linearity of time series. In literature [30], MDE and its variants were used for automatic EEG detection of epilepsy, and certain recognition effects were achieved. However, it is easy to lose information when MDE calculates the segmented average value of a coarse-grained sequence. In addition, as the scale factor is increased, the length of the coarse-grained sequence gets shorter, leading to unstable entropy value calculation results and poor accuracy, which easily reduces the recognition accuracy of different types of EEG signals [31,32].

To overcome the above shortcomings, an automatic epilepsy detection method based on improved refined composite multi-scale dispersion entropy (IRCMDE) and particle swarm optimization support vector machine (PSO-SVM) is proposed in this paper. First, the refined composite multi-scale dispersion entropy (RCMDE) is introduced, and then the segmented average value calculation of the coarse-grained sequence is replaced by the local maximum calculation to solve the problem of MDE information loss. Finally, the entropy is normalized to weaken the entropy change caused by different parameter selections and improve the entropy robustness. The above IRCMDE method is applied to the feature extraction process of the epilepsy EEG signal and combined with the advantages of the

PSO-SVM model, which is fast in computation and suitable for real-time data processing [33,34], automatic detection of epilepsy was realized. Compared with the results of MDE-PSO-SVM and RCMDE-PSO-SVM, the proposed IRCMDE-PSO-SVM method can effectively identify the normal, epileptic interictal and epileptic ictal states and is superior to the existing methods.

2. Principles and methods

2.1. Multiscale dispersion entropy

According to Eq (1), the normal cumulative distribution function is used to map the given time sequences $x_n, n = 1,2,3\ldots N$ to y_n.

$$y_n = \frac{1}{\sigma\sqrt{2\pi}}\int_{-\infty}^{x_n} e^{\frac{-(t-\mu)^2}{2\sigma^2}}\,dt \tag{1}$$

y_n is linearly transformed into the mapping set with c categories number by Eq (2).

$$z_n^c = round(c \cdot y_n + 0.5) \tag{2}$$

where $round$ is a rounding function. As shown in Eq (3), the embedding vector is reconstructed for embedding dimension m, categories number c and delay time d.

$$z_i^{m,c} = \left\{z_i^c, z_{i+d}^c, \ldots, z_{i+(m-1)d}^c\right\}, i = 1,2,\ldots N-(m-1)d \tag{3}$$

where $z_i^c = v_0, z_{i+d}^c = v_1, \ldots, z_{i+(m-1)d}^c = v_{m-1}$. $z_i^{m,c}$ are mapped to dispersion patterns $\pi_{v_0 v_1 \ldots v_{m-1}}$. $N-(m-1)d$ is the total sum of embedding vector. Therefore, the relative frequency is defined according to Eq (4).

$$p(\pi_{v_0 v_1 \ldots v_{m-1}}) = \frac{Number(\pi_{v_0 v_1 \ldots v_{m-1}})}{N-(m-1)d} \tag{4}$$

where $Number(\pi_{v_0 v_1 \ldots v_{m-1}})$ is the map number of the dispersion patterns $\pi_{v_0 v_1 \ldots v_{m-1}}$. Finally, dispersion entropy (DE) can be evaluated as shown in Eq (5).

$$DE(x,m,c,d) = -\sum_{\pi=1}^{c^m} p(\pi_{v_0 v_1 \ldots v_{m-1}})\, ln(p(\pi_{v_0 v_1 \ldots v_{m-1}})) \tag{5}$$

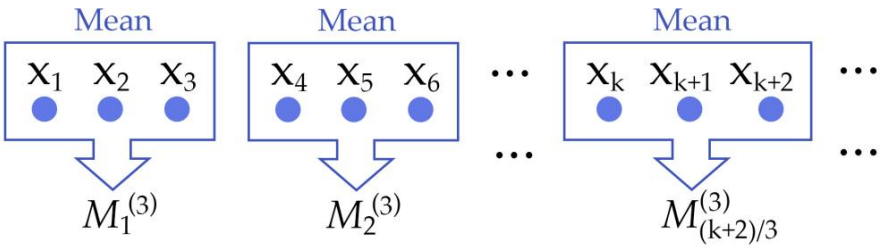

Figure 1. Schematic diagram of MDE coarse-grained process.

Figure 1 shows the coarse-grained process of the original time sequences $x_n, n = 1,2,3\ldots N$. The coarse-grained process is that the time sequence is divided into the non-overlapping windows and the data within each window is averaged. The coarse-grained time sequences are obtained as follows:

$$M_{k,j}^{(\tau)} = \frac{1}{\tau}\sum_{n=(j-1)\tau+k}^{j\tau+k-1} x_n \;\; 1 \le j \le \frac{N}{\tau}, 1 \le k \le \tau \tag{6}$$

Finally, the definition of multi-scale dispersion entropy (MDE) is formed using Eqs (5) and (6).

$$MDE(x,m,c,d,\tau) = DE(M_k^{(\tau)},m,c,d) \tag{7}$$

2.2. Improved refined composite multi-scale dispersion entropy

When performing a coarse-grained process as shown in Figure 1, MDE calculates the mean value of data points in non-overlapping windows, which leads to the "neutralization" phenomenon of the nonlinear abrupt information of the original signal, resulting in information loss. In addition, with the increase of the scale factor τ, the coarse-grained sequence becomes shorter, which leads to a decrease in entropy stability. To solve the above problems of MDE, the refined composite multi-scale dispersion entropy (RCMDE) is first introduced, and the definition of RCMDE is expressed as Eq (8).

$$RCMDE\left(M_k^{(\tau)},m,c,d,\tau\right) = \sum_{\pi=1}^{c^m} \overline{p(\pi_{v_0v_1\ldots v_{m-1}})}\, ln\left(\overline{p(\pi_{v_0v_1\ldots v_{m-1}})}\right) \tag{8}$$

As shown in Eq (9), the $\overline{p(\pi_{v_0v_1\ldots v_{m-1}})}$ is defined.

$$\overline{p(\pi_{v_0v_1\ldots v_{m-1}})} = \frac{1}{\tau}\sum_1^{\tau} p(\pi_{v_0v_1\ldots v_{m-1}}) \tag{9}$$

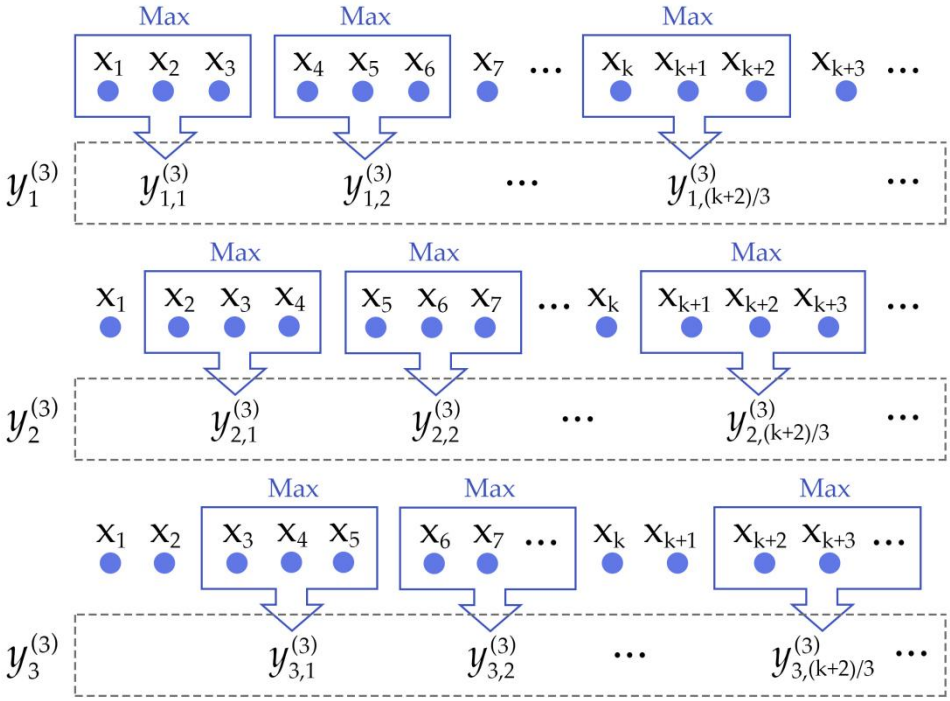

Figure 2. Schematic diagram of IRCMDE coarse-grained process.

Then, Figure 2 depicts that the segmented mean value calculation in the coarse-grained process is replaced by the local maximum calculation to avoid the problem of information loss. In addition, according to the coarse-grained process in Figure 2, the τ group sequence can be obtained to overcome the problem of coarse-grained sequence shortening and enhance the stability of the traditional multi-scale entropy algorithm. The expression for calculating the local maximum value of the coarse-grained sequence is defined as Eq (10).

$$y_{k,j}^{(\tau)} = Max(x_{(j-1)\tau+k}: x_{k+j\tau-1}),\ (1 \le j \le [N/\tau], 1 \le k \le \tau), \tag{10}$$

where Max is the maximum value calculation function.

Finally, the improved refined composite multi-scale dispersion entropy (IRCMDE) is defined and normalized as Eq (11).

$$IRCMDE(x, m, c, d, \tau) = RCMDE(y_k^{(\tau)}, m, c, d)/ln(c^m), \tag{11}$$

where $ln(c^m)$ represents the maximum value of IRCMDE.

2.3. The proposed epileptic detection scheme

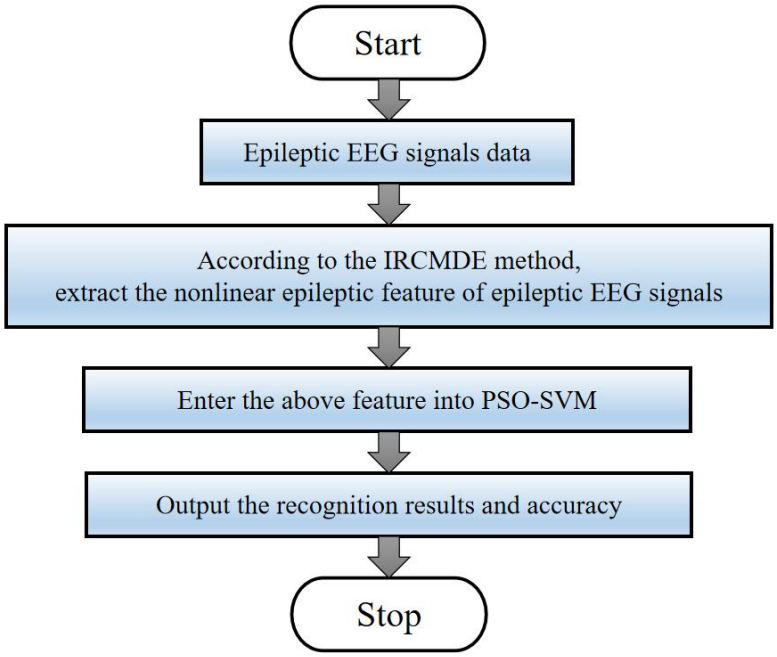

Figure 3. The flowchart of the IRCMDE-PSO-SVM epileptic detection scheme.

This section proposes a new epileptic detection method based on IRCMDE and PSO-SVM to improve the recognition accuracy of epileptic detection. The proposed IRCMDE-PSO-SVM epileptic detection scheme is depicted in Figure 3. The specific steps are as follows:

1) Epileptic EEG signals from the online database of Bonn University and CHB-MIT Scalp EEG database are used as experimental data.

2) The IRCMDE algorithm is employed to extract epileptic features from experimental data. The epileptic feature sets are randomly divided into training sample sets and test sample sets. In addition, PSO is employed to optimize the penalty factor c and kernel parameter g in SVM. The maximum population number is set as 20 and the iterations number of the PSO algorithm is set as 50. Then, the training sample sets are entered into PSO-SVM for epileptic detection model training. Finally, the IRCMDE-PSO-SVM automatic detection model of epileptic seizures is established.

3) To illustrate the effectiveness of the proposed method, the test sets are given into the PSO-SVM epileptic detection model and obtain the recognition accuracy and results. Finally, comparing the epileptic detection results of MDE-PSO-SVM, RCMDE-PSO-SVM and IRCMDE-PSO-SVM methods.

3. Results and discussion

3.1. Comparative analysis of simulated signal

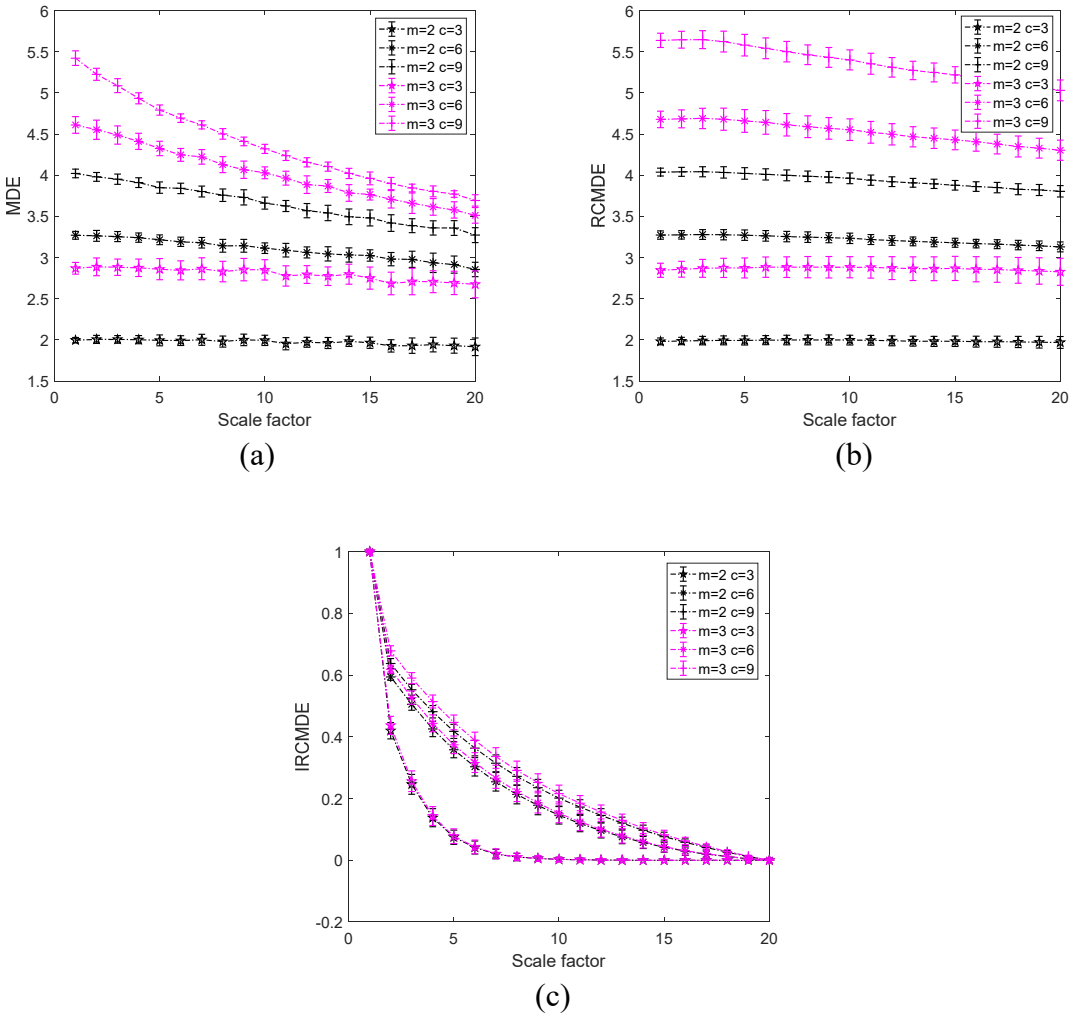

Figure 4. Mean standard deviation curves of different entropies of 1/f noise: (a) MDE; (b) RCMDE; (c) IRCMDE.

The calculation of IRCMDE is related to embedding dimension m, number of categories c and delay time d parameters. According to the literature [31], m is 2 or 3, c is an integer between 3 and 9, d is selected as 1. For illustrating the merits of the IRCMDE algorithm, the entropy performance of MDE, RCMDE and IRCMDE under different parameters will be analyzed in this section. 1/f noise is selected as the simulated signal, and Figure 4 depicts the MDE, RCMDE and IRCMDE mean standard deviation curves for the simulated signal. It is manifested from Figure 4 that the MDE and RCMDE curves of 1/f noise have an insignificant downward trend with the increase of scale factor, while the IRCMDE curve of 1/f noise has an obvious downward trend with the increase of scale factor. This means that MDE and RCMDE cannot completely extract the multi-scale information of 1/f noise, resulting in information loss. IRCMDE can better extract the multi-scale information of 1/f noise, solving the problem of information loss. Second, MDE and RCMDE curves are greatly affected by the changes of embedding dimension and number of categories, while IRCMDE curves vary little with

different embedding dimensions and number of categories, which indicates that the normalized process of IRCMDE can reduce the entropy changes caused by parameter selection and improve the robustness of features. Finally, by comparing the standard deviation of the three entropy curves, it is found that the standard deviation of RCMDE and IRCMDE is smaller than that of MDE, because the refined composite process reduces the entropy fluctuation to some extent.

3.2. Comparative analysis of EEG signal

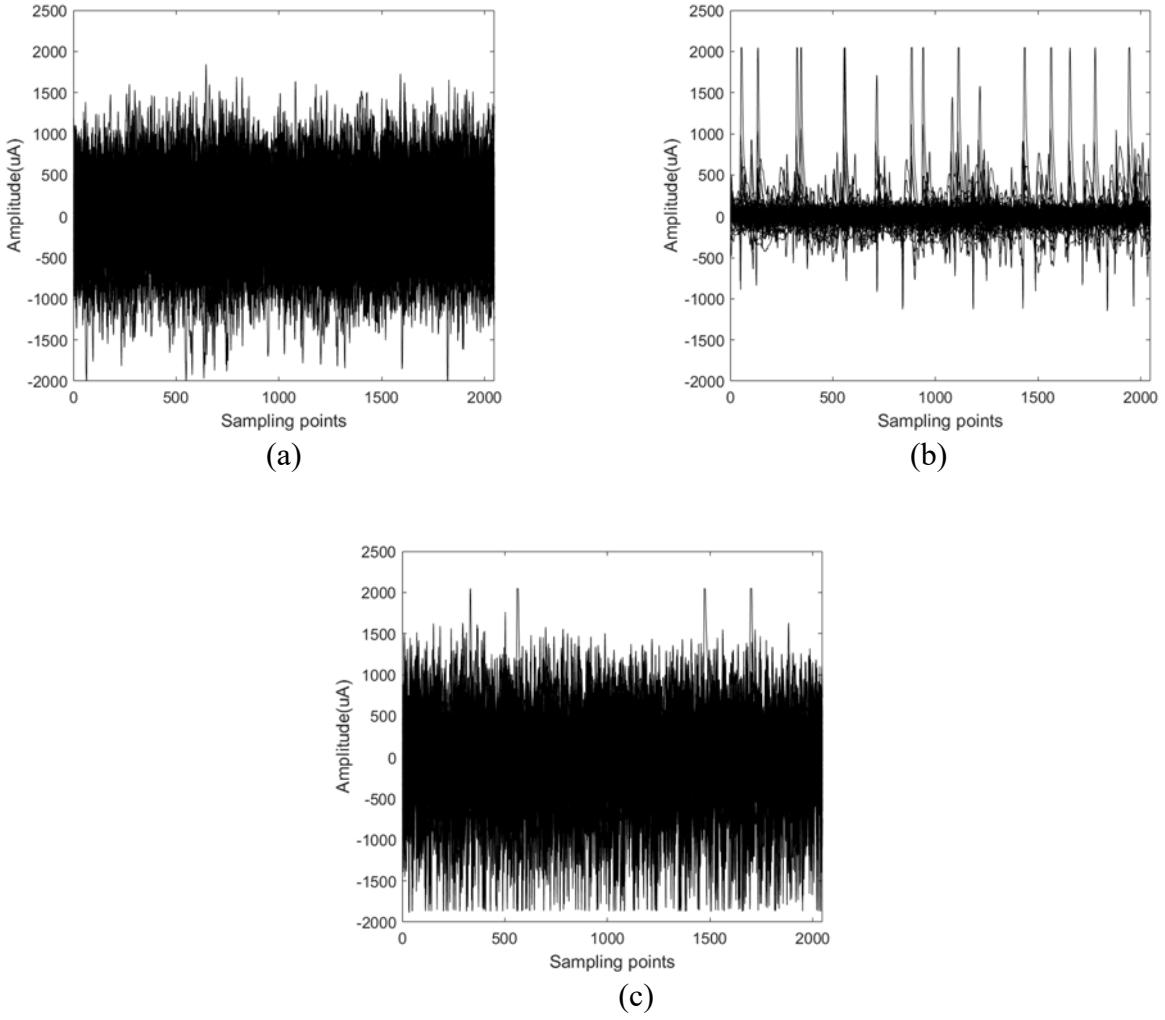

Figure 5. The EEG signal waveforms of normal (set Z), epileptic interictal (set F) and epileptic ictal states (set S): (a) normal EEG signal; (b) epileptic interictal EEG signal; (c) epileptic ictal EEG signal.

The EEG signals data used in this paper come from the epilepsy EEG signals online database of Bonn University in Germany [35]. The database contains five data sets (Z, O, N, F and S), each of which has 100 single-channel EEG segments with a duration of 23.6 seconds. A 12-bit analog-digital converter was used to digitize all EEG signal data. The sampling frequency was 173.6 Hz. Among them, data set Z is the EEG signals data collected by normal people when they open their eyes, data set F is the EEG signals data of the epileptic focal area in epileptic interictal patients, and data set S is the EEG data of the epileptic focal area in epileptic ictal patients. In this paper, EEG signals in normal,

epileptic interictal, and epileptic ictal states are automatically detected, and feature extraction and classification recognition are carried out for EEG signals data in sets Z, F and S. Figure 5 show the EEG signal waveforms of normal (set Z), epileptic interictal (set F) and epileptic ictal (set S) states with 2048 sampling points.

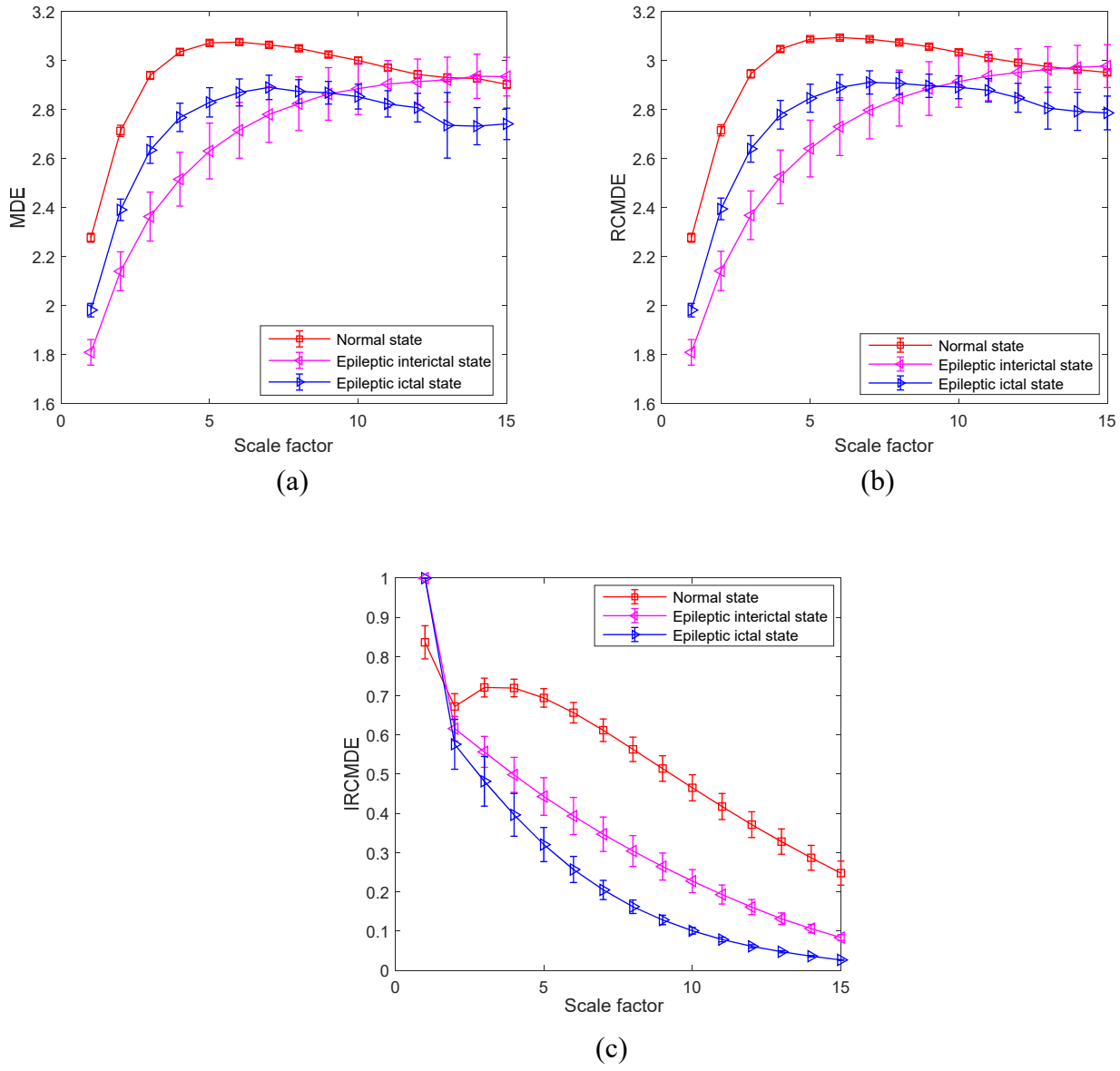

Figure 6. Mean standard deviation curves of different entropies of EEG signals in different states: (a) MDE; (b) RCMDE; (c) IRCMDE.

The entropy features of 360 EEG signals (including 120 normal EEG signals, 120 epileptic interictal EEG signals, and 120 epileptic ictal EEG signals) are extracted by MDE, RCMDE and IRCMDE methods. According to the literature [30], the embedding dimension m is selected as 3, the delay time d is 1 and the number of categories c is set to 5. We can see from Figure 6, the feature diagram of MDE, RCMDE, and IRCMDE of EEG signals in different states with scale factors 1–15 are displayed, respectively. It is manifested that the entropy values of MDE and RCMDE from EEG

signals in normal, epileptic interictal, and epileptic ictal states first increase rapidly and then decrease or become stable. The overall curve trend is consistent with that in the literature [30]. In addition, the entropy curves of EEG signals in three different states still overlap a lot, which brings great difficulty to the automatic detection and classification of epilepsy. However, the IRCMDE entropy curve can clearly distinguish the three different states at most scales, and the mean standard deviation curve of entropy value has no overlap basically. The IRCMDE can better extract the nonlinear mutation information of EEG signals. Furthermore, IRCMDE has a significantly lower standard deviation than MDE and RCMDE, which means that the proposed IRCMDE method has better stability than MDE and RCMDE.

3.3. Pattern recognition

The MDE, RCMDE and IRCMDE feature parameters extracted above are classified and recognized by the particle swarm optimization support vector machine (PSO-SVM). The 210 EEG signal data (including 70 normal, 70 epileptic interictal and 70 epileptic ictal states) were randomly assigned to the training set, while the remaining 150 EEG characteristic parameters were used as the test set. The penalty factor c and kernel parameter g in the MDE-PSO-SVM method are optimized as 1.3547 and 246.5515, respectively. The penalty factor c and kernel parameter g in the RCMDE-PSO-SVM method are optimized as 16.1814 and 159.4850, respectively. The penalty factor c and kernel parameter g in the RCMDE-PSO-SVM method are optimized as 0.9373 and 50.8685, respectively. The epilepsy classification and recognition results of MDE-PSO-SVM, RCMDE-PSO-SVM and IRCMDE-PSO-SVM are shown in Figure 7. Ordinate "1" represents the normal state, ordinate "2" represents the epileptic interictal state, ordinate "3" represents the epileptic ictal state and the abscissa is the EEG signal sample number. It is manifested that the MDE-PSO-SVM method has 12 misidentification samples, the RCMDE-PSO-SVM method has 10 misidentification samples, and the IRCMDE-PSO-SVM method only has 3 misidentification samples. The sensitivity of the MDE-PSO-SVM model to detect the epileptic interictal state is 88%, and the sensitivity of the epileptic ictal state is 90%. The sensitivity of the RCMDE-PSO-SVM model to detect the epileptic interictal state is 90%, and the sensitivity of the epileptic ictal state is 90%. The sensitivity of the IRCMDE-PSO-SVM model to detect the epileptic interictal state is 100%, and the sensitivity of the epileptic ictal state is 94%. The above results indicate the effectiveness of the proposed method. In addition, we compared the recognition rate and running time of the above three methods, as shown in Table 1. From Table 1, it can be observed that compared with the MDE-PSO-SVM and RCMDE-PSO-SVM methods, the recognition accuracy of the proposed IRCMDE-PSO-SVM automatic epilepsy detection method is higher, reaching 98%. The above results once again verify the effectiveness of IRCMDE in characterizing the nonlinear feature of epileptic EEG signals. Furthermore, IRCMDE and RCMDE approaches spend more running time compared with MDE, because the refined composite process improves the stability of the entropy value, while the process increases the calculation amount of the algorithm to a certain extent. The IRCMDE approach has a lower running time than the RCMDE due to the segmented average value calculation in the coarse-grained process being replaced by the local maximum calculation, which reduces the calculation amount and improves the algorithm running efficiency.

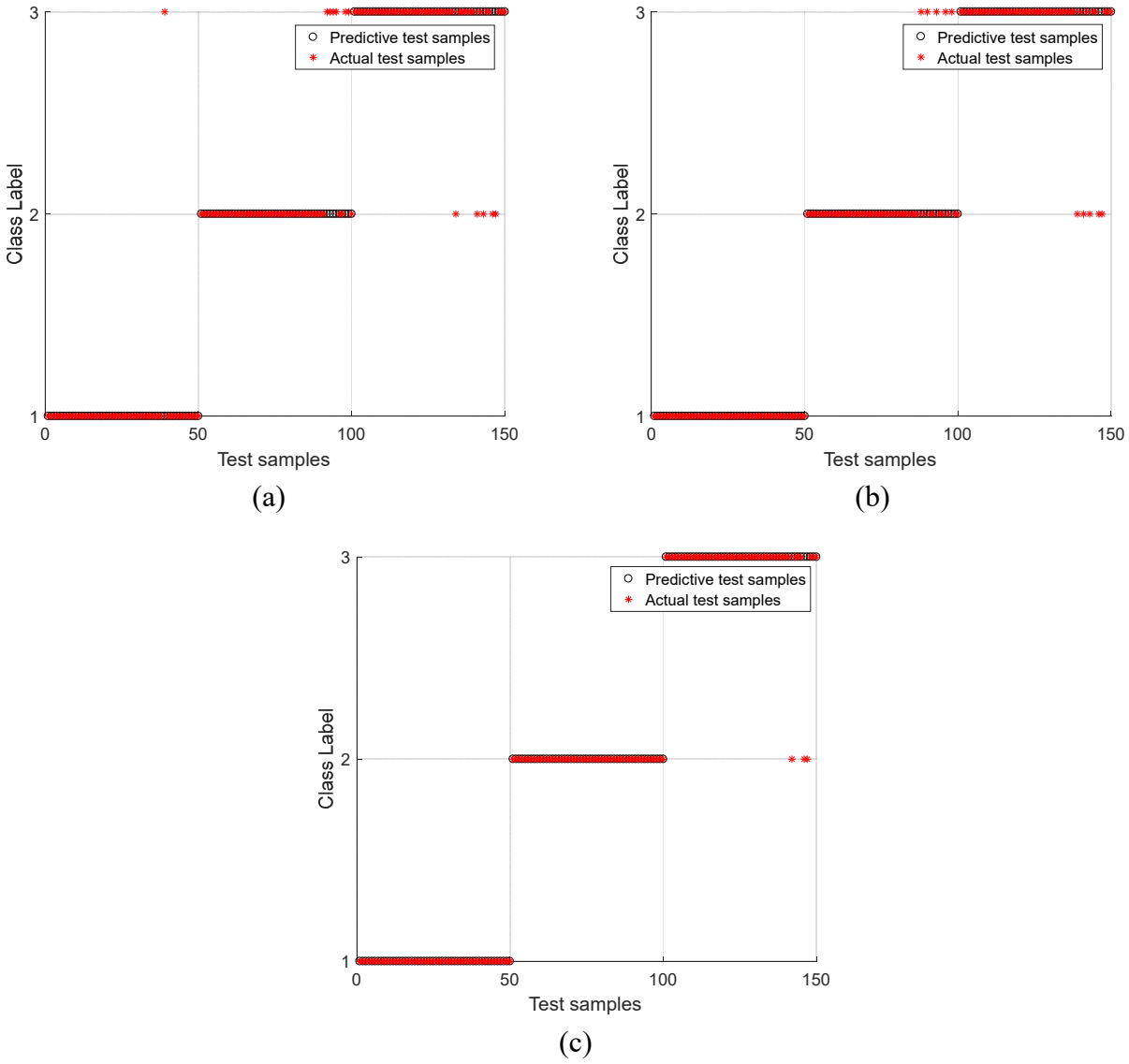

Figure 7. The epilepsy recognition results of MDE-PSO-SVM, RCMDE-PSO-SVM, and IRCMDE-PSO-SVM: (a) MDE-PSO-SVM; (b) RCMDE-PSO-SVM; (c) IRCMDE-PSO-SVM.

Table 1. Comparison of the recognition effect of different epilepsy detection methods.

Methods	Correct sample/total sample	Recognition accuracy (%)	Running time (s)
MDE-PSO-SVM	138/150	92.00	28.05
RCMDE-PSO-SVM	140/150	93.33	49.57
IRCMDE-PSO-SVM	147/150	98.00	36.35

4. Discussion

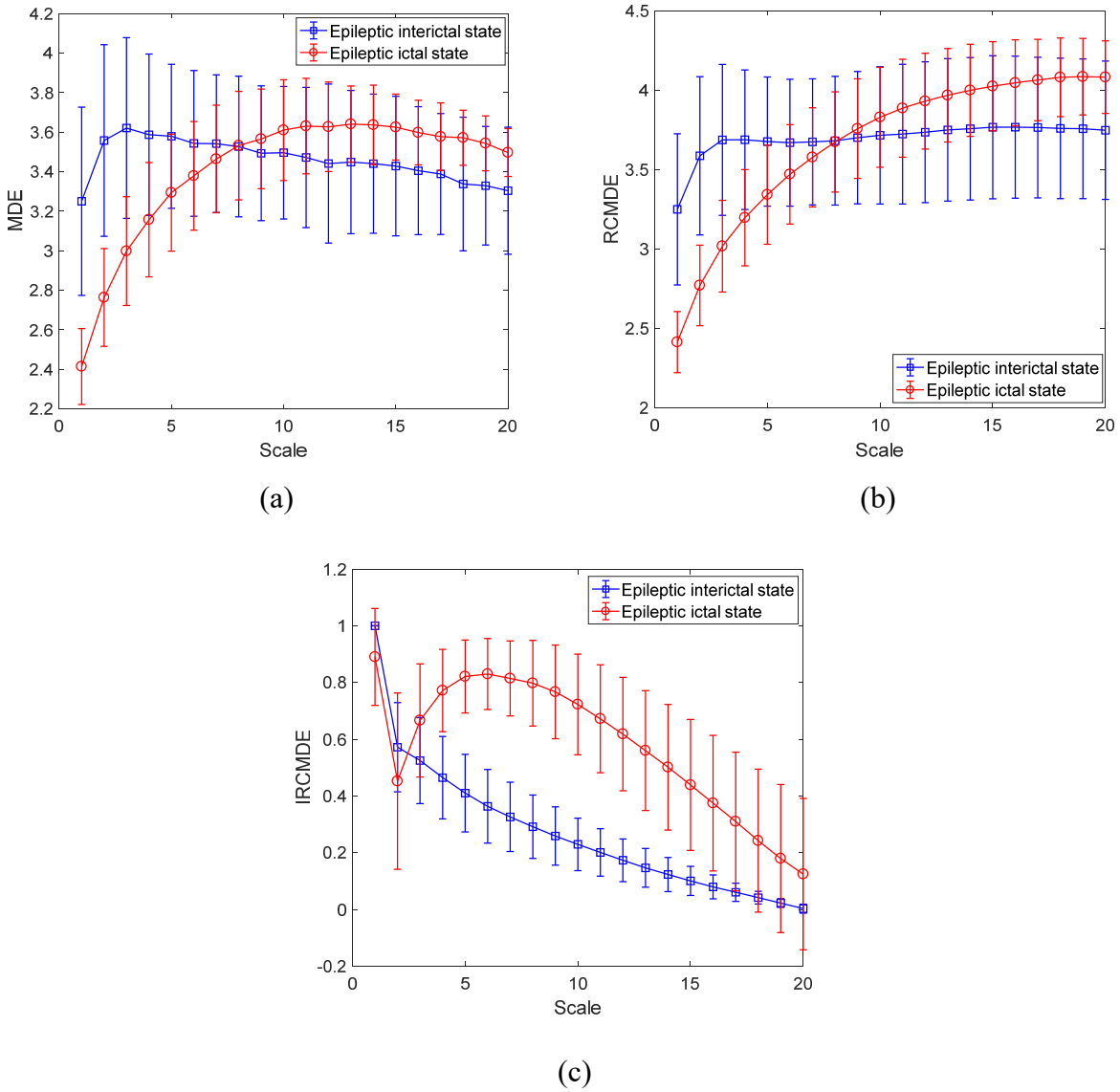

Figure 8. Mean standard deviation curves of different entropies of EEG signals from CHB-MIT Scalp EEG database: (a) MDE; (b) RCMDE; (c) IRCMDE.

In this paper, the novel IRCMDE-PSO-SVM method is proposed to realize the extraction of EEG nonlinear features and epilepsy pattern recognition. In the IRCMDE algorithm, the segmented average calculation of coarse-grained sequence is replaced by local maximum calculation to solve the problem of information loss. This is because the traditional coarse-grained process of MDE and RCMDE is shown in Figure 1. The mean value calculation is adopted in the coarse-grained process of MDE and RCMDE, which is easy to neutralize the abrupt information of the EEG signal, resulting in information loss. The coarse-grained process of IRCMDE is shown in Figure 2. The coarse-grained process of IRCMDE is calculated by the maximum value, and the new coarse-grained sequence calculated by the maximum value is approximate to the envelope of the original signal, which ensures the correctness of EEG signal information, avoids the deficiency of information loss, and can better highlight the

nonlinear characteristics of EEG signal from epileptics. In addition, the entropy value is normalized to improve the robustness of characteristic parameters. Simulated signals and actual EEG signals experiments demonstrate the superiority of this algorithm in signal feature extraction. Finally, a new intelligent epilepsy EEG automatic detection model is developed by combining the PSO-SVM algorithm, and a good recognition effect is achieved.

To further illustrate the validity of the proposed model on different epileptic EEG data sets, another CHB-MIT Scalp EEG database is used to evaluate the classification ability of the proposed model [36]. The CHB-MIT Scalp EEG database collected EEG recordings from 22 children with intractable epilepsy. We use MDE, RCMDE and IRCMDE methods to analyze 95 EEG signals of epileptic interictal and epileptic ictal states, and the results are shown in Figure 8. It can be observed that compared with MDE and RCMDE, the IRCMDE features of the two states overlap less, and can better distinguish epileptic interictal and epileptic ictal states. Combined with PSO-SVM, the binary pattern recognition is completed. The recognition rate of MDE-PSO-SVM is 83.16%. The recognition rate of RCMDE-PSO-SVM is 84.21%. The recognition rate of IRCMDE- PSO-SVM is 94.74%. The above results further prove the effectiveness of the proposed model.

However, the proposed model still has some limitations. In Table 1, the running time of the IRCMDE-PSO-SVM model reaches 36.35 seconds. Thus, the running efficiency of the proposed model needs to be improved to meet the requirements of clinical detection of epilepsy. It is planned to employ a faster and high-performance classifier in the future to reduce the running time and improve the running efficiency while ensuring a high recognition rate.

5. Conclusions

The automatic detection method of epileptic seizures based on IRCMDE and PSO-SVM is realized in this paper. The IRCMDE method is proposed to improve the inevitable disadvantages of MDE and RCMDE for time series complexity measures. The simulation results demonstrate that, compared with MDE and RCMDE, IRCMDE solves the problem of information loss when analyzing the simulation signal complexity, weakens the entropy change caused by different parameter selections, and improves the robustness of characteristic parameters. In addition, the proposed method is applied to the actual epileptic EEG signals, the results show that IRCMDE can extract nonlinear characteristics of epileptic EEG signals more effectively compared with MDE and RCMDE. The recognition accuracy of IRCMDE-PSO-SVM for epileptic detection is higher than that of MDE-PSO-SVM and RCMDE-PSO-SVM. The above results demonstrate that the proposed method can better distinguish normal, epileptic interictal, and epileptic ictal EEG signals, which provide technical support for guiding neurologists to accurately evaluate epileptic seizures.

However, while the proposed IRCMDE algorithm has been shown to be appropriate and efficacious in the automatic detection of epileptic EEG signals, it has not been proven available in other fields and requires additional experimental verification. Therefore, the writer will proceed to push forward the application of the IRCMDE algorithm in nonlinear time sequences feature extraction.

Acknowledgments

This work was supported by the Innovation and Entrepreneurship Foundation for College Students of China under grant No. 202210549005, the Excellent Young Scientist Foundation of Hunan

Provincial Education Department under grant No. 22B0694 and the Research Foundation for Advanced Talents under grant No. 21BSQD37. The authors sincerely thank the anonymous reviewers for their helpful comments and suggestions.

Conflict of interest

The authors declare there is no conflict of interest.

References

1. I. E. Scheffer, S. Berkovic, G. Capovilla, M. B. Connolly, J. French, L. Guilhoto, et al., ILAE classification of the epilepsies: position paper of the ILAE Commission for Classification and Terminology, *Epilepsia*, **58** (2017), 512–521. https://doi.org/10.1111/epi.13709
2. E. Howell, Epilepsy stigma: Moving from a global problem to a global solution, *Seizure-Eur. J. Epilepsy*, **19** (2010), 628629. https://doi.org/10.1016/j.seizure.2010.10.016
3. J. Gotman, Automatic seizure detection: improvements and evaluation, *Electroencephalogr. Clin. Neurophysiol.*, **76** (1990), 317–324. https://doi.org/10.1016/0013-4694(90)90032-F
4. F. E. Abd El-Samie, T. N. Alotaiby, M. I. Khalid, S. A. Lshebeili, S. A. Aldosari, A review of EEG and MEG epileptic spike detection algorithms, *IEEE Access*, **6** (2018), 60673–60688. https://doi.org/10.1109/ACCESS.2018.2875487
5. H. Stefan, G. Pawlik, H. G. Böcher-Schwarz, H. J. Biersack, W. Burr, H. Penin, et al., Functional and morphological abnormalities in temporal lobe epilepsy: a comparison of interictal and ictal EEG, CT, MRI, SPECT and PET, *J. Neurol.*, **234** (1987), 377–384. https://doi.org/10.1007/BF00314081
6. S. Raghu, N. Sriraam, Y. Temel, S. V. Rao, A. S. Hegde, P. L. Kubben, Complexity analysis and dynamic characteristics of EEG using MODWT based entropies for identification of seizure onset, *J. Biomed. Res.*, **34** (2020), 213. https://doi.org/10.7555/JBR.33.20190021
7. U. R. Acharya, S. V. Sree, G. Swapna, R. J. Martis, J. S. Suri, Automated EEG analysis of epilepsy: a review, *Knowledge-Based Syst.*, **45** (2013), 147–165. https://doi.org/10.1016/j.knosys.2013.02.014
8. S. Altunay, Z. Telatar, O. Erogul, Epileptic EEG detection using the linear prediction error energy, *Expert Syst. Appl.*, **37** (2010), 5661–5665. https://doi.org/10.1016/j.eswa.2010.02.045
9. M. K. Siddiqui, R. Morales-Menendez, X. Huang, N. Hussain, A review of epileptic seizure detection using machine learning classifiers, *Brain Inf.*, **7** (2020), 1–18. https://doi.org/10.1186/s40708-020-00105-1
10. U. R. Acharya, H. Fujita, V. K. Sudarshan, S. Bhat, J. E. Koh, Application of entropies for automated diagnosis of epilepsy using EEG signals: A review, *Knowledge-Based Syst.*, **88** (2015), 85–96. https://doi.org/10.1016/j.knosys.2015.08.004
11. A. Bhattacharyya, R. B. Pachori, A. Upadhyay, U. R. Acharya, Tunable-Q wavelet transform based multiscale entropy measure for automated classification of epileptic EEG signals, *Appl. Sci.*, **7** (2017), 385. https://doi.org/10.3390/app7040385
12. S. Patidar, T. Panigrahi, Detection of epileptic seizure using Kraskov entropy applied on tunable-Q wavelet transform of EEG signals, *Biomed. Signal Process.*, **34** (2017), 74–80. https://doi.org/10.1016/j.bspc.2017.01.001

13. U. R. Acharya, F. Molinari, S. V. Sree, S. Chattopadhyay, K. H. Ng, J. S. Suri, Automated diagnosis of epileptic EEG using entropies, *Biomed. Signal Process.*, **7** (2012), 401–408. https://doi.org/10.1016/j.bspc.2011.07.007
14. H. Ocak, Automatic detection of epileptic seizures in EEG using discrete wavelet transform and approximate entropy, *Expert Syst. Appl.*, **36** (2009), 2027–2036. https://doi.org/10.1016/j.eswa.2007.12.065
15. V. Gupta, R. B. Pachori, Epileptic seizure identification using entropy of FBSE based EEG rhythms, *Biomed. Signal Process.*, **53** (2019), 101569. https://doi.org/10.1016/j.bspc.2019.101569
16. P. Sharanreddy, P. K. Kulkarni, EEG signal classification for epilepsy seizure detection using improved approximate entropy, *Int. J. Public Health Sci.*, **2** (2013), 23–32. https://doi.org/10.11591/ijphs.v2i1.1836
17. H. Luo, T. Qiu, C. Liu, P. Huang, Research on fatigue driving detection using forehead EEG based on adaptive multi-scale entropy, *Biomed. Signal Process.*, **51** (2019), 50–58. https://doi.org/10.1016/j.bspc.2019.02.005
18. Y. Song, J. Crowcroft, J. Zhang, Automatic epileptic seizure detection in EEGs based on optimized sample entropy and extreme learning machine, *J. Neurosci. Meth.*, **210** (2012), 132–146. https://doi.org/10.1016/j.jneumeth.2012.07.003
19. J. Xiang, C. Li, H. Li, R. Cao, B. Wang, X. Han, et al., The detection of epileptic seizure signals based on fuzzy entropy, *J. Neurosci. Meth.*, **243** (2015), 18–25. https://doi.org/10.1016/j.jneumeth.2015.01.015
20. G. Ouyang C. Dang, X. Li, Multiscale entropy analysis of EEG recordings inepileptic rats, *Biomed. Eng: Appl. Basis Commun.*, **21** (2009), 169–176. https://doi.org/10.4015/S1016237209001222
21. C. Bandt, B. Pompe, Permutation entropy: a natural complexity measure for time series, *Phys. Rev. Lett.*, **88** (2002), 174102. https://doi.org/10.1103/PhysRevLett.88.174102
22. W. P. Yao, T. B. Liu, J. F. Dai, J. Wang, Multiscale permutation entropy analysis of electroencephalogram, *Acta. Phys. Sin.*, **63** (2014), 78704. https://doi.org/10.7498/aps.63.078704
23. B. Liu, W. Tan, X. Zhang, Z. Peng, J. Cao, Recognition study of denatured biological tissues based on multi-scale rescaled range permutation entropy, *Math. Biosci. Eng.*, **19** (2022), 102–114. https://doi.org/10.3934/mbe.2022005
24. L. Y. Zhao, L. Wang, R. Q. Yan, Rolling bearing fault diagnosis based on wavelet packet decomposition and multi-scale permutation entropy, *Entropy*, **17** (2015), 6447–6461. https://doi.org/10.3390/e17096447
25. Y. Gao, F. Villecco, M. Li, W. Song, Multi-scale permutation entropy based on improved LMD and HMM for rolling bearing diagnosis, *Entropy*, **19** (2017), 176. https://doi.org/10.3390/e19040176
26. B. Fadlallah, B. Chen, A. Keil, J. Principe, Weighted-permutation entropy: A complexity measure for time series incorporating amplitude information, *Phys. Rev. E*, **87** (2013), 22911. https://doi.org/10.1103/PhysRevE.87.022911
27. B. Liu, S. Qian, W. Hu, Identification of denatured biological tissues based on time-frequency entropy and refined composite multi-scale weighted permutation entropy during HIFU treatment, *Entropy*, **21** (2019), 666. https://doi.org/10.3390/e21070666

28. R. Li, J. Wang, Interacting price model and fluctuation behavior analysis from Lempel-Ziv complexity and multi-scale weighted-permutation entropy, *Phys. Lett. A*, **380** (2016), 117–129. https://doi.org/10.1016/j.physleta.2015.09.042
29. M. Rostaghi, H. Azami, Dispersion entropy: a measure for time-series analysis, *IEEE Signal Process. Lett.*, **23** (2016), 610–614. https://doi.org/10.1109/LSP.2016.2542881
30. M. Chakraborty, D. Mitra, Automated detection of epileptic seizures using multiscale and refined composite multiscale dispersion entropy, *Chaos Solitons Fractals*, **146** (2021), 110939. https://doi.org/10.1016/j.chaos.2021.110939
31. J. Zheng, H. Pan, Q. Liu, K. Ding, Refined time-shift multiscale normalised dispersion entropy and its application to fault diagnosis of rolling bearing, *Physica A*, **545** (2020), 123641. https://doi.org/10.1016/j.physa.2019.123641
32. H. Azami, M. Rostaghi, D. Abasolo, J. Escudero, Refined composite multiscale dispersion entropy and its application to biomedical signals, *IEEE Trans. Biomed. Eng.*, **64** (2017), 2872–2879. https://doi.org/10.1109/TBME.2017.2679136
33. X. Dai, K. Sheng, F. Shu, Ship power load forecasting based on PSO-SVM, *Math. Biosci. Eng.*, **19** (2022), 4547–4567. https://doi.org/10.3934/mbe.2022210
34. Y. Huang, J. Luo, Z. Ma, B. Tang, K. Zhang, J. Zhang, On combined PSO-SVM models in fault prediction of relay protection equipment, *Circuits Syst. Signal Process.*, **42** (2023), 875–891. https://doi.org/10.1007/s00034-022-02056-w
35. R. G. Andrzejak, K. Lehnertz, F. Mormann, C. Rieke, P. David, C. E. Elger, Indications of nonlinear deterministic and finite-dimensional structures in time series of brain electrical activity: Dependence on recording region and brain state, *Phys. Rev. E*, **64** (2001), 61907. https://doi.org/10.1103/PhysRevE.64.061907
36. A. Shoeb, H. Edwards, J. Connolly, B. Bourgeois, S. T. Treves, J. Guttag, Patient-specific seizure onset detection, *Epilepsy Behav.*, **5** (2004), 483–498. https://doi.org/10.1016/j.yebeh.2004.05.005

AIMS Press

©2023 the Author(s), licensee AIMS Press. This is an open access article distributed under the terms of the Creative Commons Attribution License (http://creativecommons.org/licenses/by/4.0)